Realization of a Solid-Propellant based Microthruster using Low Temperature Co-fired Ceramics

Jaya THAKUR[1], Rudra PRATAP[1], Yannick FOURNIER[2], Thomas MAEDER[2], Peter RYSER[2]

[1] Department of Mechanical Engineering, Indian Institute of Science, Bangalore-560012, India, pratap@mecheng.iisc.ernet.in

[2]Laboratoire de Production Microtechnique, Ecole Polytechnique Fédérale de Lausanne, CH-1015 Lausanne, Switzerland

Received: 21 May 2010 /Accepted: 21 June 2010 /Published: 25 June 2010

Abstract: The introduction of micro-spacecraft in the space industry has led to the development of various micro-propulsion techniques. Microthrusters are micropropulsion devices used in microspacecraft for precise station keeping, orbit adjustment, attitude control, drag compensation and apogee kicking. The principle of operation of a solid propellant thruster is based on the combustion of a solid energetic material stored in a microfabricated chamber. In the current work, Low-Temperature Co-fired Ceramic (LTCC) technology has been used for the realization of a solid propellant based microthruster structure. Hydroxyl Terminated Poly-Butadiene/Ammonium Perchlorate (HTPB/AP) is used as the propellant. It is shown that geometric and dimensional variations in design, depending on the application requirements, can be easily implemented. Preliminary testing for micro-combustion has been done to verify the basic operation of the microthruster. A thrust value of 19.5 mN has been measured.

Keywords: LTCC, MEMS, thrust, solid propellant, micropropulsion

1. Introduction

Existing satellites weighing in the range of few tonnes are launched using massive rockets that cost immensely. Miniaturization of spacecraft has notable advantages such as reduction in the cost of launch, increase in the reliability of mission by incorporating redundancy and reduction of development time. Change of mission trajectory or payload during the development phase calls for major changes in the design of conventional propulsion systems using the present-day technology. Changes required in a system of microspacecraft for a similar change during development phase are comparatively minor.

Propulsion is a key factor in the miniaturization of spacecraft, because microspacecraft would need very small but accurate forces and impulses to realize stabilization and station keeping. Mueller et. al. [1, 2] point out that for a satellite of mass less than 20 kg, 10^{-6} N·s to 10^{-4} N·s of impulse is required to maintain its pointing attitude, depending on the required pointing accuracy and time interval between thruster firings. The precise level of thrust and impulse required for microspacecraft applications cannot be reached with conventional propulsion systems that are too big and consume a lot of power.

Micropropulsion has been an active area of research for the last two decades. Technological efforts are being made for the development of new mechanisms and miniaturization of conventional thrusters. Most of these efforts use MEMS technology for their realization. There are various kinds of propulsion systems under investigation, a few of them being cold gas thrusters, bi-propellant thrusters [3], vaporizing liquid thrusters [4], micro ion thrusters, FEEP (Field Emission Electric Propulsion) [5], digital microthrusters [6, 7], resistojet thrusters [8], pulsed plasma thrusters [9] and Hall-effect thrusters.

Solid propellant microthruster is a comparatively new class of micropropulsion system. It offers various advantages over other propulsion systems. For example, the system complexity is minimized as there are no pumps and valves involved. This eliminates the frictional losses due to absence of moving parts. Solid propellants are generally stable over time and can be stored at room temperature.

The main constraint with this type of devices is the lack of restart ability, which can be partially compensated by deploying an array of them with suitable addressing electronics. Researchers have been able to develop single-shot solid-propellant based micro-rocket array thrusters on a single substrate [10-15]. This also makes the system highly redundant and flexible. In case of failure of a few thrusters, other thrusters in the array would still be able to satisfy the mission requirements. The number of thrusters can be adapted according to the duration or number of times the propulsion system will have to be used in a specific mission, whereas the size of thrusters in an array can be tailored to obtain the level of micro-thrust required. Individual or sequential firing of the thrusters in the array will ensure controlled and vectored levels of thrust.

Research groups working on solid propellant based microthrusters have come up with different architectures. These can be broadly categorized into the sandwich configuration, building block design and LTCC based design. The sandwich configuration [16] comprises 3 layers of silicon, with layers acting as combustion chamber, micro-nozzle and a polysilicon resistor, that acts as an igniter. In the building block design [17], the chamber, the convergent-divergent nozzle and the ignition slot are fabricated simultaneously on the same layer of silicon and a wire is used as an igniter, which is suitable for integration and batch production. The LTCC-based design [18] retains the advantages of the building block design and offers a few advantages over the silicon structure. LTCC structures are also suitable for batch production, are more reliable and have better ignition efficiency due to the embedded igniter in place of the wire igniter. High-aspect ratio structures with vertical walls can be easily obtained in LTCC due to the layering concept. Also, the thermal properties of LTCC can be tailored based on the requirements. This technology is more economical than silicon MEMS (microelectromechanical systems), as it does not require expensive clean-room processes for the realization of the structure.

The main raw material used in LTCC fabrication is the unfired "green" tape, e.g. glass-ceramic dielectric powder joined by an organic binder [19]. In this state, the material can be easily shaped and patterned by mechanical and laser cutting. LTCC combines the inherently multilayer capability of High-Temperature Co-fired Ceramic (HTCC) technology with the processing advantages of "classical" thick-film technology, i.e. the use of Ag- and Au-based conductors, and firing in a standard air atmosphere below 950°C [20]. Furthermore, passive elements such as resistors, capacitors and inductors may be easily embedded using special thick-film and/or tape materials [21]. In contrast, HTCC, whose tape material is based on alumina, requires firing at ca. 1500°C in H_2:H_2O atmosphere with Mo- or W-based conductors [19] and does not feature such an extensive set of functional materials.

Due to this outstanding combination of properties, LTCC has recently seen developments beyond pure electronics, in the fields of sensors, microfluidics and biomedical applications [22, 23]. Therefore, it was selected for the fabrication of the device presented in this work.

2. Layout and Fabrication

The principle of operation of a solid-propellant based microthruster is very simple. A solid energetic material is stored in a micro machined chamber which, upon ignition, burns and produces gases that are accelerated through an adapted nozzle to produce a thrust.

The proposed LTCC solid propellant microthruster is fabricated by the lamination of individually processed layers of green tapes. The number of tapes we have used is either six or eight depending on the design; the design of each layer is decided by the structure of the microthruster. The microthruster contains a cavity (combustion chamber), a convergent-divergent nozzle and a resistor embedded inside the cavity (Fig. 1). Due to the major role played by the igniter in the successful functioning of the device, special attention was paid to its design to achieve a successful ignition. In order to minimize the power consumption and reduce the thermal losses to the substrate, some variants of microthrusters had their resistor insulated from the LTCC substrate by using a sacrificial layer of an experimental paste compatible with LTCC. This concept had been used successfully by Briand et al. for the realization of suspended microheaters [27].

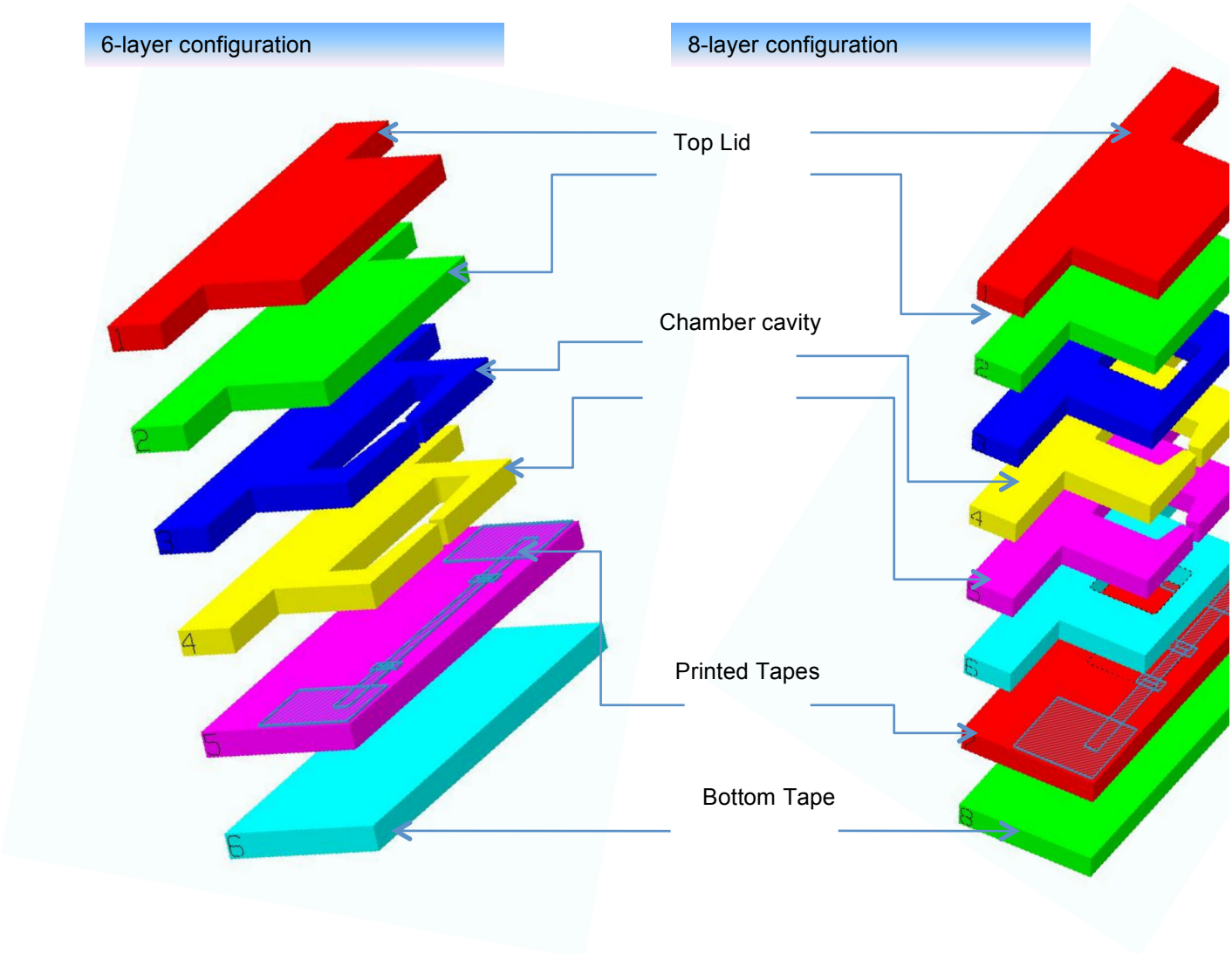

Fig. 1. Schematic models of LTCC microthrusters

In the 6-layered configuration, the top two layers serve as a lid of required thickness for sustaining the pressure inside the chamber. The next double layer with the cavity and the nozzle geometry cut along

the tapes form the height of the microcavity, giving it a depth of 420 µm. The fifth layer has the resistor and conductor printed on it. The bottom-most layer is a blank layer provided to prevent the collapse of cavity and sustain the combustion pressure. In the 8-layered configuration, two extra layers are added, one each on either side of the microcavity layers. This is done to study the effect of increasing the chamber cross-sectional area on the performance of the thruster, keeping the throat and the exit areas the same.

In the present work, the selection of conductor and resistor pastes was made using the product selector guide for DuPont (DP) 951 Green Tape™, and based on previous work at EPFL [24]. Tapes DP 951C2 - 2 mil (50.8µm) and DP 951AX - 10 mil (254µm) thick are used. DP 6146 Ag/Pd paste is used as the conducting composition, as it also adequately fulfils the role of resistor termination material and provides a surface suitable for assembly and interconnection by soldering and wire bonding. Compositions DP 5092D and DP CF011 are used as resistors. The sacrificial paste is an experimental composition consisting of a carbon paste in organic solvents [25].

Realization of the final device structure involves the following three major steps.

i) Preparation of drawings:

An area of 65 mm x 65 mm on the raw tape was available to accommodate several possible variants of the design. We selected 12 variants, 4 numbers of each kind on each tape (Fig. 2). The variants were fabricated to study the effect of variations in (a) the chamber and nozzle geometry (b) the type of resistor, (c) the resistor geometry, and (d) the presence or not of a sacrificial layer under the resistor. Design and drawing of the variants was done using HYDE, a commercial hybrid design software from Durst CAD/CONSULTING GmbH, which interfaces with the laser machine for cutting tapes (via HPGL files), and with high-resolution plotters for preparation of screens for thick-film screen printing of conductor and resistor inks (via GERBER file). In order to achieve the final desired dimensions after firing, the software compensates the shrinkage due to the sintering of the ceramic, around 14% in X and Y directions based on our previous studies, by scaling up the design dimensions accordingly.

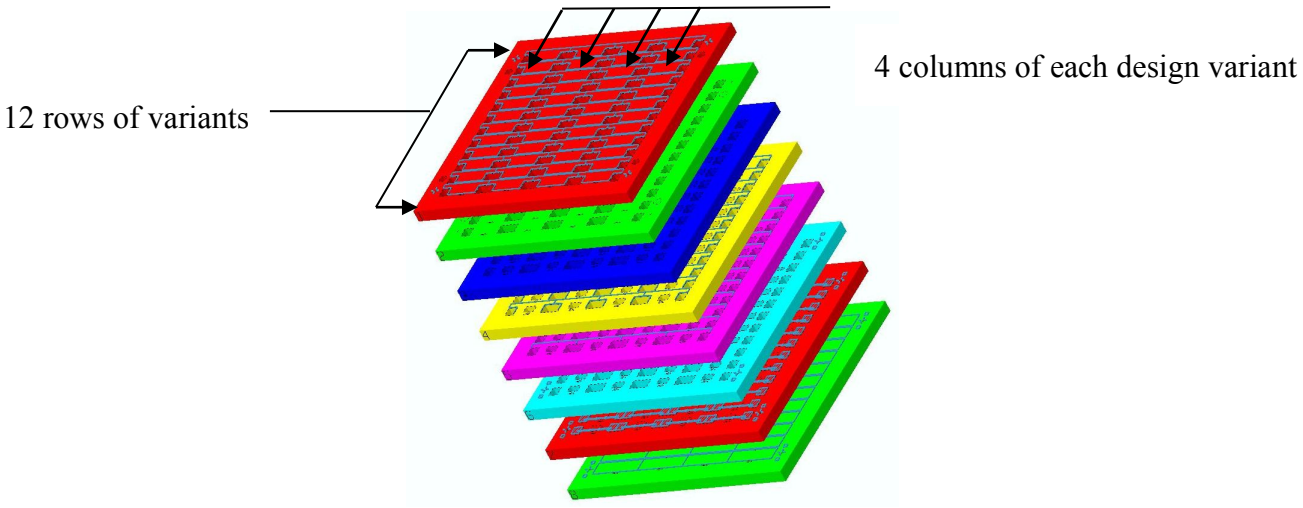

Fig. 2. Arrangement of design variants on tapes (8-layered configuration)

ii) Structure fabrication:

Fabrication of the LTCC structure involves a sequence of steps. The LTCC tapes are supplied in a very flexible state. A Mylar backing is provided to the tapes for easy handling and also to prevent premature drying. This backing is removed by hand and the tapes are pre-conditioned in a box-furnace for 20-30 minutes at 120˚C or at room temperature for 24 hours, in order to relieve internal stresses. This is

followed by laser cutting on a LS9000 trimming-laser machine. Using laser drilling, the cavities and registration holes for visual alignment during screen-printing are created in the tapes, with registration holes cut in every layer for alignment purposes. Stamp-like separation lines are also added in the design, providing an easy way to individualize the thrusters by breaking up the plate after firing. In addition, a small cut is also made at the exit of the nozzles to provide a reproducible geometry there, i.e. to keep the small inherent variability of the breaking process from affecting the flow of gases at the exit. Fig. 3 shows the laser separation lines and the cavity at nozzle exit on tape number 4.

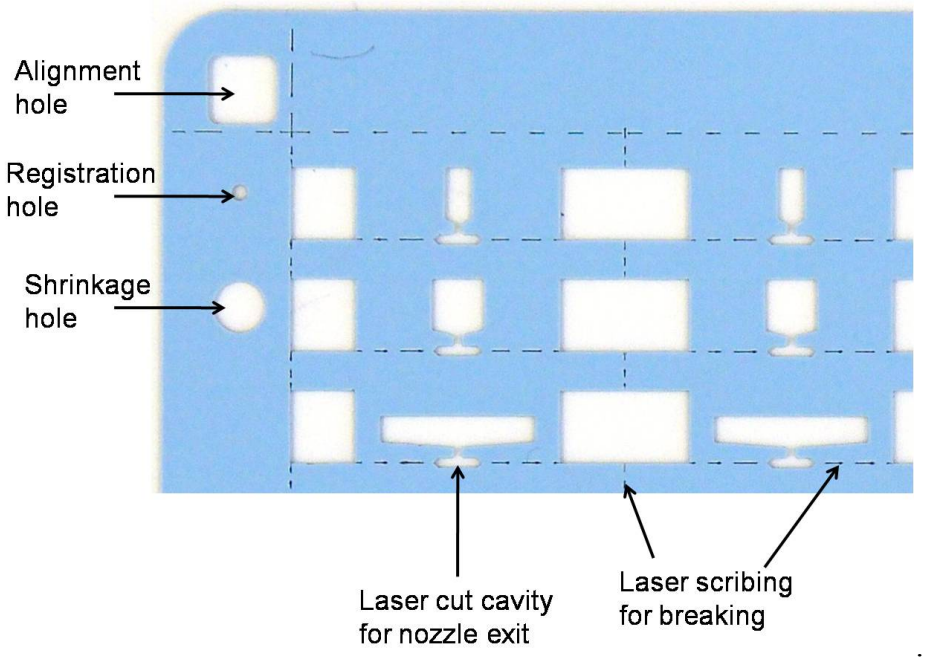

Fig. 3. Details of tape #4 after laser cutting.

The designed thick-film sacrificial material, conductor and resistor layers were screen printed (in the indicated order, Fig. 5) on the tape using an Aurel C900 semi-automatic screen-printer, fitted with an optical alignment system and a porous stone vacuum chuck to hold the ceramic tape in place. The corresponding screens were of the standard mesh/emulsion type (325 meshes/inch, ca. 78 µm/mesh; 40 µm photosensitive emulsion thickness). Compared to standard thick-film technology, screen-printing on unfired LTCC tapes is found to give slightly better final resolution, due to inhibition of paste spreading by the porosity of the tape, combined with the slight magnification of the print needed to compensate the sintering shrinkage.

After printing, the inks were first allowed to settle 5 min at room temperature, then dried in a ventilated oven at 120˚C for 10 minutes. Each print was inspected after drying. Then the tapes were inspected under a microscope. The same procedure was applied for printing the sacrificial layer, followed by printing the resistor (DP CF011 or DP 5092D). Step 3 of Fig. 4 shows the tape after the printing of resistors.

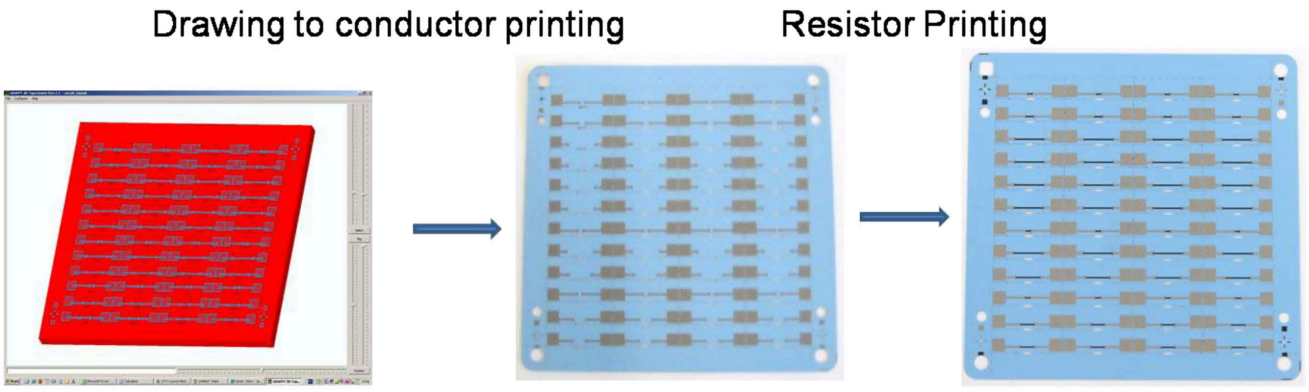

Fig. 4. Screen-printing steps: Step-1: Preparation of drawing in HYDE, Step-2: Screen-printing of the metallization layer, Step-3: Screen-printing of resistor.

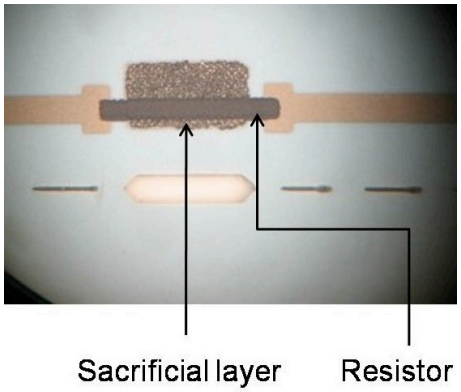

Fig. 5. Screen-printed resistor, showing the layer sequence (version with sacrificial layer).

After the processing of all the layers is completed, they are stacked in a laminating fixture and layer to layer alignment is ensured. The fixture uses alignment pins into which the registration holes of all the layers fit (Fig. 6). Lamination is done using a uni-axial hydraulic press. The pressure is calculated based on the area of the LTCC tape on which the pressure acts (excluding the cavities).

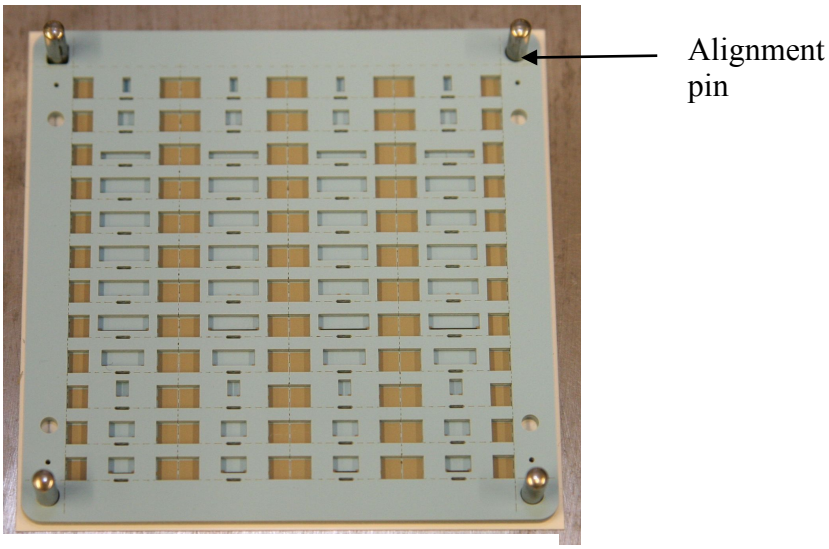

Fig. 6. Lamination and stacking of tapes

The next step is the firing of the laminated stack in a programmable box furnace ATV PEO 601. The furnace is programmed to follow the temperature-time profile for the firing process. The stack is placed on a quartz tray and heated according to the programmed temperature profile (in air, peak ca. 20 min at 875°C). The profile is chosen in accordance with the type of material, resistor and sacrificial layer being fired, with thick LTCC modules needing longer binder burnout times. After firing, the stack is manually broken along the laser scribed lines to individualize thrusters (Fig.7). Soldering of ignition wires is then done at 250˚C by preheating the co-fired thrusters on a hot plate to maintain the substrate at a sufficiently high temperature. This step has to be done before filling the cavity with propellant, as the ignition temperature of the propellant lies too close to that of the soldering step..

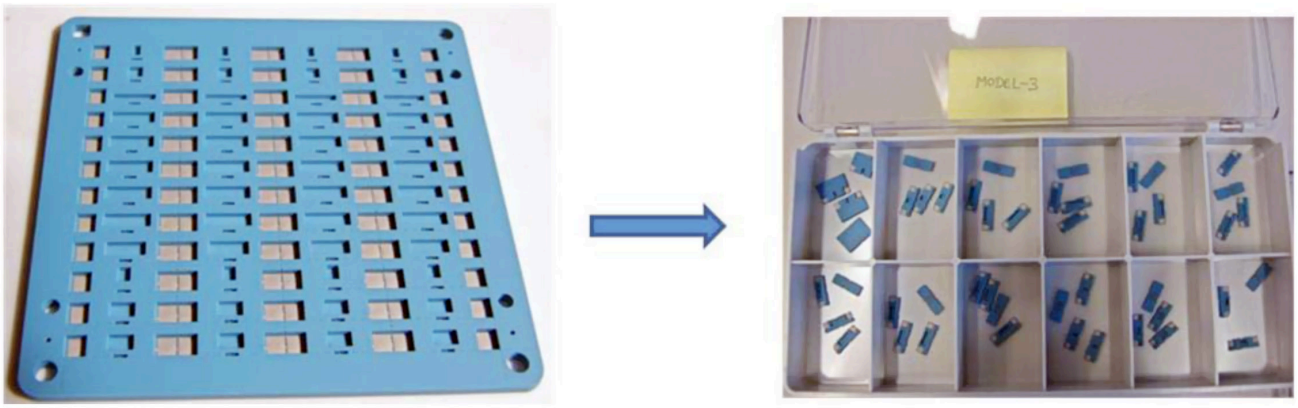

Fig. 7. Cutting of the co-fired circuit into individual thrusters

iii) Propellant filling:

Propellant filling is a very crucial step in the realization of the microthruster. Cavity-free filling of a pasty propellant into blind holes featuring a substantial aspect ratio is difficult. Air trapped in the hole or cavity is a limitation when injected with a very viscous product. The propellant is dispensed into the small cavities using a syringe dispenser system driven by compressed air. The viscosity of the propellant ensures it flows to all parts of the chamber, including the resistor area, yielding cavity-free filling to some extent. Due to the elasticity of the propellant, it has to be handled carefully to avoid spilling on the walls of the chamber. The loaded propellant mass affects the LTCC microthruster performance in terms of specific impulse. Consequently, the propellant mass should be controlled and measured strictly before testing. The weight of the propellant in the chamber ranges from 4.7 to 14 mg for various chamber geometries.

The final step in the realization of the microthruster is gluing the lid; this was preferred to soldering the lid due to the risk of igniting the propellant accidentally; the ignition temperature of the propellant is expected to be in the range of 250-350°C. The glue has to be strong enough to withstand the pressure (20 bars) and temperature increase generated by combustion of gases inside the chamber. cyanoacrylate and Loctite 3430 epoxy were initially used for gluing, but could not withstand the conditions of combustion. Then EpoTek 353 ND-T epoxy [55] was successfully used for testing thrusters. This glue was applied on the whole surface of the top of the wall, the lid was applied to close the chamber, and the assembly was cured for 2 hours at 100°C. Figure 8 shows a thruster after the curing of the glue and ready for testing.

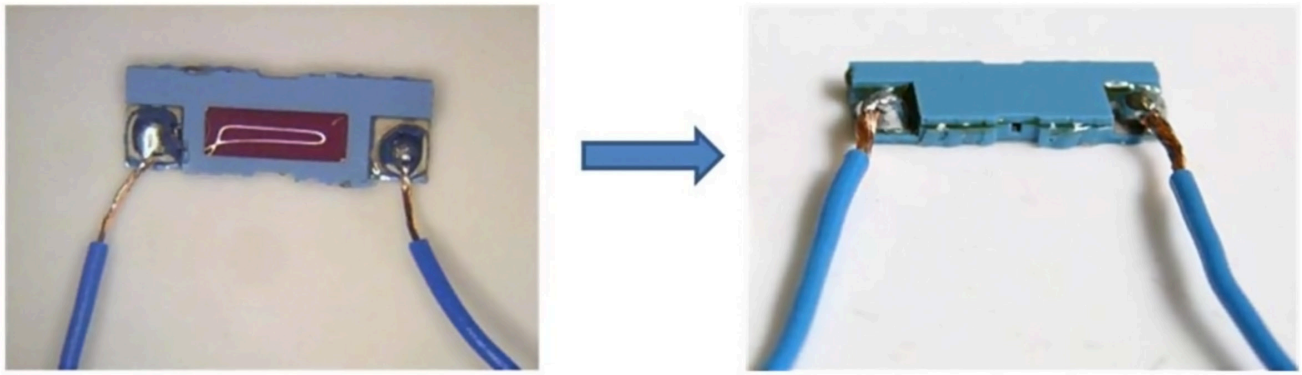

Fig. 8. Propellant filling and gluing steps. The exhaust nozzle is clearly visible in the center on the right image.

3. Testing and Results

Unfortunately, none of the resistors screen printed over sacrificial layer presented a proper shape after the LTCC circuit firing. As Fig. 9 can attest, strong buckling deformations can be observed at the extremities, close to the resistor terminations. There can be two reasons to this drawback: a) a possible chemical incompatibility of our sacrificial paste with the resistor, or (more probably) b) the resistor having no contact with the substrate upon sintering, and its own shrinkage being lower than the one of LTCC tape, it suffered from compression at its extremities that resulted in strong buckling. Of course the resistor is useless with this out-of-plane shape: it is higher than the cavity, and would have been crushed at the time of filling the propellant anyway. Therefore, only the non-sacrificial versions of the microthrusters were further processed, which nevertheless allowed ignition due to the localised heating and low thermal conductivity of LTCC.

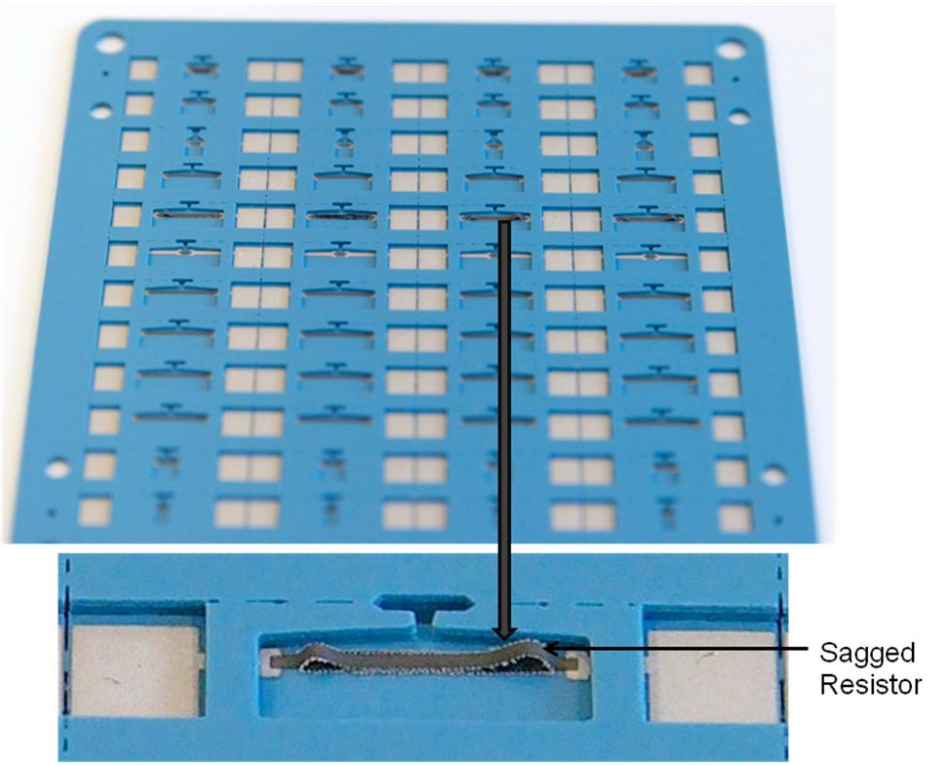

Fig. 9. Failed attempt to make free-standing resistors using CF011 resistor paste.

Control of the propellant ignition process in a microthruster is of critical importance for its applications. The repeatability of the temperature produced has to be ensured for reliable functioning of the microthruster. Characterization of the resistors was done using a power supply, a multimeter and an infra-red camera. Several trials were carried out to establish the proper heating power to ensure ignition and to check the resistor failure mode when overheated. In this case, failure was always found to occur at the centre of the resistor for the different studied variants, indicating reproducible ignition characteristics (Fig. 10).

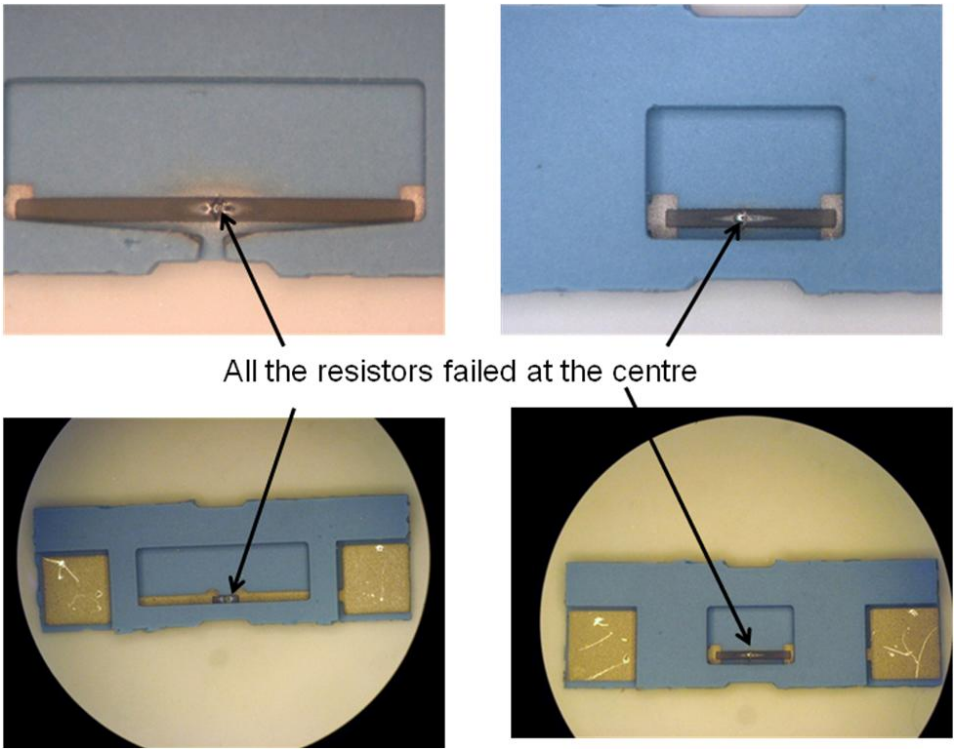

Fig. 10. Failure of overheated resistors (versions without sacrificial layer).

Preliminary combustion testing is done to check the integrity of the structure. Successful firing of the thruster was obtained after a few initial failures. Fig.11 (left) shows the picture of a structure that failed while testing its structural integrity. The thickness of the wall was subsequently modified to take care of the pressure levels. Another issue was failure due to insufficient strength of the glue bond, which occurred sporadically even after changing to the stronger EpoTek 353 ND-T epoxy (Fig. 11, right): the dimensioning of the device must therefore be adjusted so that the adhesively bonded surfaces are large enough.

Fig. 11. A failed microthruster due to insufficient wall thickness (left) and glue bond strength (right).

An experimental set-up was made to test the viability of the design and acquire the characteristics of the LTCC solid propellant microthruster at near sea level (ca. 400 m). The setup consisted of a high-speed digital video camera to capture the propellant microcombustion, a MilliNewton force sensor [26], a fixture to facilitate the positioning of the thruster on the sensor, an oscilloscope and a DC power supply (Fig. 12). LabView software was used to capture the data on the computer.

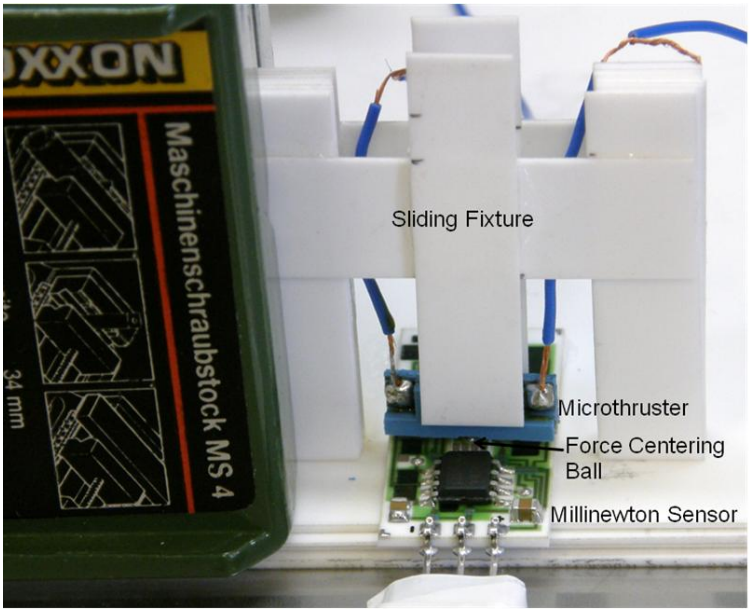

Fig. 12. Mechanical jig used to hold the microthrusters and measure their thrust force.

Fig. 13 shows a typical result of a microthruster test captured on the computer. This model with an A_c/A_t (ratio of chamber and throat cross-sectional areas) of 60 and A_e/A_t (ratio of exit and throat cross-sectional areas) of 40 was successfully tested for the measurement of thrust. The length of the chamber was 1000 microns and semi-diverging angle 10˚. From the signal images shown in the figure, the duration of combustion is recorded as 150 ms, and an average thrust of 19.5 mN is measured.

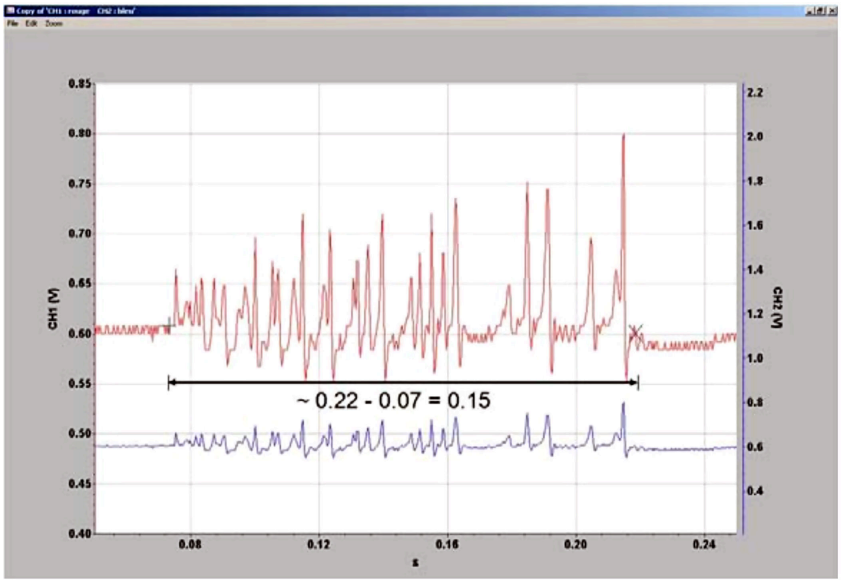

Fig. 13. Screen-capture of the measurement of thrust on oscilloscope

x-axis : Time in seconds, y-axis : Thrust in Volts

4. Conclusions

In the present study, the design and fabrication of LTCC microthrusters has been demonstrated and discussed. This type of microthruster has high-level integration, better ignition efficiency and reliability, adjustable thermal characteristics and more design freedom compared to silicon based solid-propellant microthrusters. Effect of nozzle geometry, chamber geometry, resistor design has been studied to obtain different thrust and impulse levels. An LTCC-based solid propellant microthruster has been successfully tested to generate a thrust of 19.5 mN at an altitude of ca. 400 m.
It must be mentioned that only one iteration of design/fabrication could be done in the allotted time-frame of this project. In their current state, the microthrusters can only be reliably fired with the help of the mechanical jig, which plays a role of pressure container by preventing the lid from exploding during the propellant ignition. However we have no doubt that a slight increase of thicknesses of the walls, of the lid and of the glue bond will be sufficient to suppress mechanical failures upon firing.
Regarding the propellant, we observed that it had tendency to expand and spill out of the nozzle during the curing of the epoxy. This can be corrected by employing adhesives with lower curing temperatures or by fine tuning the propellant compounds proportions upon mixing.

Acknowledgements

Fabrication and testing of the hardware was supported by the Laboratoire de Production Microtechnique (LPM) of the Ecole Polytechnique Fédérale de Lausanne (EPFL), Switzerland. The authors also acknowledge the partial financial support from the EPFL-India research collaboration program.

References

[1]. J. Mueller, C. Marrese, J. Polk, E.-H. Yang, A. Green, V. White, D. Bame, I. Chakraborty, S. Vargo, An overview of MEMS based micropropulsion development at JPL, In *Proceedings of 3rd IAA Symposium on 'Small Satellites for Earth Observation'*, Berlin, Germany, 2001.
[2]. J. Mueller, Thruster Options for Microspacecraft: A Review and Evaluation of State-of-the-Art and Emerging Technologies, Micropropulsion for Small Space-craft, *Progress in Astronautics and Aeronautics* 187 (2000), pp. 45-137.
[3]. A. P. London, A. A. Ayon, A. H. Epstein, S. M. Spearing, T. Harrison, Y. Peles and Cambridge USA J. L. Kerrebrock. Microfabrication of a high pressure bipropellant rocket engine, *Sensors and Actuators A* 92 (2001), pp. 351-357.
[4]. E. V. Mukherjee**,** A. P. Wallace, K. Y. Yan, D. W. Howard, R. L. Smith and S. D. Collins. Vaporizing liquid microthrusters, *Sensors Actuators* 83 (2000), pp. 231-236.
[5]. S. W. Janson. Chemical and electrical micropropulsion concept for nanosatellite, In *Proceedings of the 30th AIAA/ASME/SAE/ASSEE Propulsion Conference*, pp. 199-199.
[6]. D.H. Lewis Jr., S.W. Janson, R.B. Cohen and Erik K. Antonsson**,** Digital micropropulsion, *Sensors Actuators* 80 (2000)pp.143-154.
[7]. L. Stenmark, Y. Backlund, J. Kohler, K. Larsson, U. Simu, Micropropulsion thrusters for space application, *Micro structure Workshop*, 1998.
[8]. M.N. Sweeting, Low cost orbit maneuvers for minisatellites using novel resistojets thrusters, In *Proceedings of the Conference on 'Instr. Mech. Eng.'* 213, 1999.
[9]. R.J Cassady, W.A Hoskins, M Campbell, C Rayburn, A micropulsed plasma thruster (PPT) for the 'Dawgstar' Spacecraft, *IEEE*, 4(2000) pp. 7-14.
[10]. H. L. David Jr., W. J. Siegfried, B. C. Ronald and K. A. Erik. Digital Micropropulsion, *Sensors and Actuators A* 80(2000), pp. 143-154.
[11]. W. Y. Daniel, T. L. Son, C. Edgar, B. N. Jamie, E. B. Robert, J. G. Kenneth, F. Dave, L. Rodney and Z. Xiaoyang, MEMS Mega-pixel Micro-thruster Arrays for Small Satellite Stationkeeping,

In *Proceedings of the 14th Annual/USU Conference on 'Small Satellites'*, North Logan, U.S.A., 2000.
[12]. C. Rossi, S. Orieux, B. Larangot, T. D. Conto and D. Esteve, Design, fabrication and modeling of solid propellant microrocket-application to micropropulsion, *Sensors and Actuators A* 99 (2002), pp. 125-133.
[13]. T. Shuji, H. Ryuichiro, T. Shinichiro, H. Keiichi, S. Hirobumi, W. Masashi and E. Masayoshi, MEMS-Based Solid Propellant Rocket Array Thruster with Electrical Feedthroughs, *Trans. Jpn Soc. Aero. Space Sci*., 46 (51) (2003), pp. 47-51.
[14]. C. Rossi, B. Larangot, P.Q. Pham, D. Briand, N.F. de Rooij, M. Puig-Vidal, J. Samitier, A. Chaalane, Solid propellant microthrusters on silicon: design, modeling, fabrication and testing, *Journal of Micro-Electro-Mechanical Systems*, 15 (2006), pp. 1805-1815.
[15]. K. L. Zhang, S. K. Chou and S. A. Simon, Development of a solid propellant microthruster with chamber and nozzle etched on a wafer surface, *J. Micromech. Microeng*.14 (2004), pp. 785-792.
[16]. C. Rossi, T. D. Conto, D. Esteve and B. Larangot, Design, fabrication and modeling of MEMS-based microthrusters for space application, *Smart Materials and Structures* 10 (2001), pp. 1156-1162.
[17]. Z. Kaili, S. K. Chou and S. S. Ang, MEMS-Based Solid Propellant Microthruster Design, Simulation, Fabrication and Testing, *Journal of Microelectromechanical Systems* 13(2) (2004).
[18]. K. L. Zhang, S. K. Chou and S. S. Ang, Development of a low-temperature co-fired ceramic solid propellant microthruster, *Journal of Micromechanics and Microengineering* 15 (2005), pp. 944-952.
[19]. R.R. Tummala, Ceramics in microelectronic packaging, *American Ceramic Society Bulletin* 67:4 (1988), pp. 752-758.
[20]. M. Monneraye, Les encres sérigraphiables en microélectronique hybride: les matériaux et leur comportement [Screen-printable inks in hybrid microelectronics: the materials and their behaviour], *Acta Electronica* 21:4 (1978), pp. 263-281.
[21]. A. H. Feingold, M. Heinz, R. L. Wahlers, M. A. Stein, Materials for capacitive and inductive components integrated with commercially available LTCC systems, in *Proceedings, 3rd Annual Conference on Microelectronics and Packaging, IMAPS-Israel, Herzelia, Israel* (2003).
[22]. E. G. Palmer and C. M. Newton, 3-D packaging using low-temperature co-fired ceramic (LTCC), *Int. J. Microcircuits Electron. Packag.* 16 (1993), pp. 279-284.
[23]. M. R. Gongora-Rubio, P.Espinoza-Vallejos, L. Sola-Laguna, J. J. Santiago-Aviles, Overview of low temperature co-fired ceramics tape technology for meso-system technology (MsST), *Sensors Actuators A* 89 (2001), pp. 222-241.
[24]. Y. Fournier, G. Boutinard-Rouelle, N. Craquelin, T. Maeder, P. Ryser, SMD pressure and flow sensor for compressed air in LTCC technology with integrated electronics, *Procedia Chemistry - Proceedings of Eurosensors XXIII* 1:1 (2009), pp. 1471-1474.
[25]. H. Birol, T. Maeder, P. Ryser, Application of graphite-based sacrificial layers for fabrication of LTCC (low temperature co-fired ceramic) membranes and micro-channels, *Journal of Micromechanics and Microengineering* 17 (2007), pp. 50-60.
[26]. T. Maeder, V. Fahrny, S. Stauss, G. Corradini, P. Ryser, Design and characterisation of low-cost thick-film piezoresistive force sensors for the 100 mN to 100 N range, in *Proceedings, XXIX International Conference of IMAPS Poland, Koszalin* (2005), pp. 429-434.
[27]. Danick Briand, Phuong Quyen Pham and Nicolaas F. de Rooij, Reliability of freestanding polysilicon microheaters to be used as igniters in solid propellant microthrusters", *Sensors and Actuators A, vol. 135*, pp. 329-336, 2007.
